Sbds is required for Rac2-mediated monocyte migration and signaling downstream of RANK during osteoclastogenesis

Roland Leung,[1] Karl Cuddy,[1] Yongqiang Wang,[1] Johanna Rommens,[2] and Michael Glogauer[1]

[1]Matrix Dynamics Group, University of Toronto, Toronto, ON; and [2]Hospital for Sick Children, Program in Genetics and Genome Biology, Toronto, ON

Shwachman-Diamond syndrome (SDS) results from mutations in the *SBDS* gene, characterized by exocrine pancreatic insufficiency and hematologic and skeletal abnormalities. Neutropenia and neutrophil dysfunction are hallmark features of SDS; however, causes for the bone defects are unknown. Dysfunction of bone-resorbing osteoclasts, formed by the fusion of monocytic progenitors derived from the same granulocytic precursors as neutrophils, could be responsible. We report that Sbds is required for in vitro and in vivo osteoclastogenesis (OCG). Sbds-null murine monocytes formed osteoclasts of reduced number and size because of impaired migration and fusion required for OCG. Phenotypically, Sbds-null mice exhibited low-turnover osteoporosis consistent with findings in SDS patients. Western blotting of Rho GTPases that control actin dynamics and migration showed a 5-fold decrease in Rac2, whereas Rac1, Cdc42, and RhoA were unchanged or only mildly reduced. Although migration was rescued on Rac2 supplementation, OCG was not. This was attributed to impaired signaling downstream of receptor activator of nuclear factor-κB (RANK) and reduced expression of the RANK-ligand-dependent fusion receptor DC-STAMP. We conclude that Sbds is required for OCG by regulating monocyte migration via Rac2 and osteoclast differentiation signaling downstream of RANK. Impaired osteoclast formation could disrupt bone homeostasis, resulting in skeletal abnormalities seen in SDS patients. (*Blood*. 2011;117(6): 2044-2053)

Introduction

Shwachman-Diamond syndrome (SDS) is an autosomal recessive disorder with hallmark features of bone marrow failure, exocrine pancreatic insufficiency, and skeletal abnormalities.[1-3] Neutropenia is the most common clinical manifestation of bone marrow failure, but patients may also experience pancytopenia, anemia, and thrombocytopenia, and be at increased risk of developing aplastic anemia and acute myeloid leukemia.[4] In early cross-sectional studies, metaphyseal dysostosis was observed in 40% to 80% of SDS patients, and rib and/or thoracic cage abnormalities in 30% to 50% of SDS patients.[5-7] More recently, in a longitudinal study, all of the SDS patients studied displayed various skeletal abnormalities, including delayed appearance of secondary ossification centers, variable widening, and irregularity of the metaphyses in early childhood followed by progressive thickening and irregularity of the growth plates, and generalized osteopenia.[8] In addition, a subset of patients showed early signs of osteoporotic vertebral deformities and disturbances in bone homeostasis manifesting in low-turnover osteoporosis.[8,9] Oral and dental diseases and conditions, including periodontitis, delayed eruption of the permanent dentition, increased caries risk in primary and permanent dentitions, and increased soft tissue pathoses, have also been reported.[10]

SDS results from mutations in the ubiquitously expressed, conserved Shwachman-Bedian-Diamond syndrome gene (*SBDS*).[11] The exact function of the SBDS protein remains unclear; however, in recent years, through studies of orthologs in yeast and Archaea[12,13] and patient bone marrow cells,[14-16] it has been postulated to function in RNA metabolism and ribosome biogenesis. *SBDS* is an essential gene in embryogenesis,[17] and SBDS has also been implicated in cell division[18,19] and cellular stress responses.[20]

In addition to concerns of neutropenia and recurrent infections, neutrophils of affected persons have been shown to exhibit impaired chemotaxis and deficiency in migration.[21,22] A less-characterized abnormality with SDS patients is their defect in bone homeostasis, a parameter that is normally maintained via the balanced activities of bone-producing osteoblasts and bone-resorbing osteoclasts.[23] A unique feature of osteoclast formation, or osteoclastogenesis (OCG), involves multiple fusions of pre-osteoclasts derived from cells from the monocyte-macrophage lineage, a process requiring a dynamic actin cytoskeleton that is regulated by small GTPases.[24,25] Two critical ligands, receptor activator of nuclear factor-κB ligand (RANKL) and macrophage-colony stimulating factor (M-CSF), are essential for OCG: mice with ablated genes for RANKL or its receptor, RANK, are completely devoid of osteoclasts.[26] Further, the addition of RANKL and M-CSF to cells of the mononuclear phagocyte lineage in vitro is sufficient for the generation of mature functional osteoclasts.[25] Because both neutrophils and monocytes are derived from the same myeloid granulocyte progenitors, and neutrophil numbers and function are impaired in SDS, osteoclasts may also be negatively affected resulting in an uncoupling of bone formation/resorption and loss of bone homeostasis.

The objective of this study is to investigate whether SBDS is required for in vitro and in vivo OCG, and if so, the possible mechanisms involved, using mice with conditional Sbds-ablation only in granulocytes, and an in vitro OCG model we previously established.[27,28]

Submitted April 28, 2010; accepted October 28, 2010. Prepublished online as *Blood* First Edition paper, November 17, 2010; DOI 10.1182/blood-2010-05-282574.

The publication costs of this article were defrayed in part by page charge payment. Therefore, and solely to indicate this fact, this article is hereby marked "advertisement" in accordance with 18 USC section 1734.

Methods

Animals and isolation of bone marrow monocytes

All procedures were performed in accordance with the *Guide for the Humane Use and Care of Laboratory Animals* and were approved by the University of Toronto Animal Care Committee. Mice containing conditional (S^c) and null *Sbds* alleles (S^-) were generated as described.[17] Ablation of Sbds in mature myeloid lineages were obtained by breeding mice heterozygous for the Sbds alleles ($S^{c/+}$ and $S^{-/+}$) to those with *Cre* recombinase under control of the *LysM* promoter[29,30] ($L^{Cre/Cre}$), to obtain $S^{c/-}L^{Cre/Cre}$ mutant (Sbds-null) and $S^{c/+}L^{Cre/Cre}$ control (wild-type [WT]) genotypes. Mice were maintained on a mixed BL6/SV129 background. DNA was extracted from tail specimens to establish genotypes. Polymerase chain reaction (PCR) genotyping was performed by amplification with primers located in intron 1 of Sbds (5′AAACTGAGGCAGGAGGATTG and 5′CCCTGGAAAATGACCATAATGT) to detect S^+(WT) and S^c (conditional) alleles with fragments of 484 and 399 bp, respectively. The S^- and L^{Cre} alleles were identified as described.[17,30]

To isolate bone marrow osteoclast precursors (monocytes), tibia and femora from 8- to 12-week-old mice were dissected aseptically under a laminar air flow hood, and cells were processed and isolated as previously described.[27] Monocytes were resuspended in α-minimal essential medium supplemented with 10% fetal bovine serum and antibiotics (164 IU/mL penicillin G, 50 μg/mL gentamicin, and 0.25 μg/mL Fungizone) at 0.5×10^6 cells/mL.

OCG

Monocytes were induced to form osteoclasts by plating 5×10^4 cells/well in a 6-well tissue culture plate supplemented with 20 ng/mL M-CSF (M9170, Sigma-Aldrich) and 60 ng/mL recombinant murine sRANKL (PeproTech). Cells were cultured for 6 days, with a change of cell culture media and cytokine supplementation every second day. To evaluate the effect of increased initial cell density on OCG, WT and Sbds-null monocytes were also plated at 2.5×10^5 cells/well and grown for 6 days. On day 6, cells were washed twice with phosphate-buffered saline (PBS), fixed with 4% paraformaldehyde, and stained for tartrate-resistant acid phosphatase (TRACP). Fixed cells were incubated in a solution of naphthol AS-BI phosphate and fast red TR salt (Sigma-Aldrich) in 0.2M acetate buffer (pH 5.2) containing 100mM sodium tartrate (Sigma-Aldrich) for 10 minutes at 37°C and subsequently washed twice with water. Red-stained cells were viewed with a Leitz Wetzlar microscope (original magnification ×200, 20×/0.32 objective), and images were taken with a PixeLink camera and processed using PixeLink Release 3.2 software (Vitana Corp.). The number of TRACP-positive osteoclasts and the number of nuclei within these osteoclasts were counted in 10 random fields of view.

Histology and DXA analysis of the mouse skeleton

Dual-energy x-ray absorptiometry (DXA) was performed on 12-week-old female mice after CO_2 asphyxiation, using an animal PIXImus densitometer (Lunar; GE). Data for bone mineral density (BMD) and bone mineral content (BMC) were collected for the lumbar vertebrae, left femur, and the entire skeleton after masking of the heads, as well as percentage body fat, by a single operator. Femurs for histology and subsequent TRACP staining were processed as previously described[27] using standard histologic methods. Osteoclasts were quantified in 3 histologic sections per mouse and expressed as mean osteoclast per bone section. Osteoclasts were visualized using a Nikon Eclipse E1000 microscope with a Plan Apo 40×/0.95 DiC M lens and a Plan Fluor 10×/0.30 DiC L lens; images were taken with a Hamamatsu ORCA-ER camera and processed using Simple PCI software (Version 5.2.1.1609; Compix Inc).

Transwell (Boyden chamber) migration assay

Monocyte migration was evaluated using Transwell permeable supports with 5 μm membrane pores in a 24-well plate (Corning Life Sciences), as previously described.[27] These inserts were first incubated in α-minimal essential medium growth medium for 30 minutes at 37°C, after which 0.5×10^6 cells (in 200 μL) were added to the Transwell insert and incubated for 2 hours at 37°C to allow for cell attachment to the membrane. Nonadherent cells were removed, and the inserts were placed in 600 μL growth medium alone or supplemented with M-CSF (20 or 100 ng/mL) and further incubated for 2 hours at 37°C to allow for migration. The inserts were then fixed in 4% paraformaldehyde, stained with 0.165μM 4′6,-diamidino-2-phenylindole (Sigma-Aldrich), and washed thoroughly with PBS. Cells adhered to the top of the membrane but had not migrated through the membrane were removed by gentle wiping with a cotton swab and rinsing with PBS, and the membranes were cut out from the inserts and mounted onto glass slides for counting of cell nuclei. Cell nuclei in 10 random fields of view per sample were counted manually using a Nikon Eclipse E400 fluorescent microscope (original magnification ×200).

Western blotting

At the indicated time points, monocytes/osteoclasts in culture were washed twice with PBS and lysed with 100 μL ice-cold RIPA buffer (Sigma-Aldrich) supplemented with 1mM phenylmethylsulfonyl fluoride and 1 times protease inhibitor (BD Pharmingen) for 5 minutes and collected by cell scraping. Cell lysates were centrifuged for 1 minute at 15 000*g* to pellet cellular debris; 5 × Laemmli sample buffer was added to the lysates and boiled for 10 minutes. Samples were subjected to sodium dodecyl sulfate-polyacrylamide gel electrophoresis using a 12% polyacrylamide gel, transferred onto nitrocellulose membrane (GE Healthcare), and immunoblotting was performed as previously described.[27] Immunoreactive protein was detected using chemiluminescence with ECL Plus (GE Healthcare) on exposure to Bioflex MSI film (Clonex). Band intensities on scanned films were quantified by densitometry using Image J Version 1.41 software and normalized against β-actin levels used as internal loading controls. Proteins in Sbds-null cells were presented as proportions of WT. Primary antibodies used were as follows: goat polyclonal anti-Sbds (S-15, Santa Cruz Biotechnology; 1:100); rabbit polyclonal anti-c-Fms/CSF-1R (C-20, Santa Cruz Biotechnology; 1:600); goat polyclonal anti-RANK (M-20, Santa Cruz Biotechnology; 1:600); mouse monoclonal anti-Rac1 (23A8, Upstate Biotechnologies; 1:2000); rabbit polyclonal anti-Rac2 (Upstate Biotechnologies; 1:5000); mouse monoclonal anti-RhoA (26C4, Santa Cruz Biotechnology; 1:200); and mouse monoclonal anti-Cdc42 (B-8, Santa Cruz Biotechnology; 1:100). Secondary antibodies used were as follows: Horseradish peroxidase-conjugated sheep anti–mouse IgG (610-603-002, Rockland; 1:4000 for Rac1, 1:1000 for Cdc42, 1:2000 for RhoA); horseradish peroxidase-conjugated donkey anti–rabbit IgG (NA934V, GE Healthcare; 1:2000); and horseradish peroxidase-conjugated rabbit anti–goat IgG (Alpha Diagnostic International; 1:2000).

TAT protein constructs and rescue of migration and OCG

Constructs of TAT fusion proteins for protein transduction were kindly provided by the late Dr Gary Bokoch (Scripps Research Institute, La Jolla, CA). TAT fusion proteins for WT and constitutively active (CA) Rac2 (G12V), Rac1-CA (G12V), and empty vector pTAT-HA were produced and purified as described.[27] We previously determined optimal TAT fusion protein entry into monocytes with a maximal level after 10 minutes, and a protein concentration of 500nM, which is comparable with conditions used by others.[31,32] To observe the effects of TAT fusion proteins on migration, cells were preincubated for 10 minutes before being added to Transwell supports, and migration assays was performed as described in the Transwell migration assay section above. When used in OCG rescue experiments, fresh culture media containing TAT proteins (500nM), RANKL, and M-CSF were changed daily for 6 days.

Evaluation of the RANK signaling pathway

To investigate whether signaling downstream of RANK was intact in Sbds-null cells, activation of Nuclear Factor kappa B (NF-κB) and nuclear factor of activated T cells c1 (NFATc1), 2 transcription factors crucial for OCG, was measured and compared with activation of c-Jun, which is not essential. Activation of the transcription factors NF-κB and c-Jun was

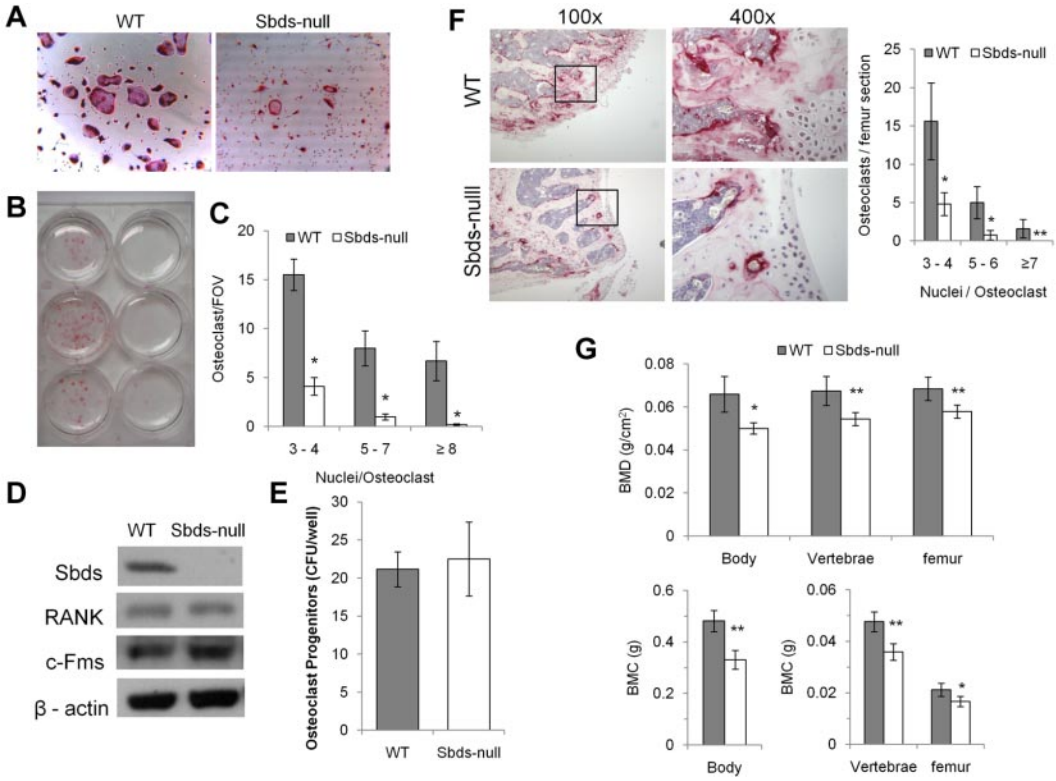

Figure 1. Sbds is required for in vitro and in vivo OCG. (A) Photomicrographs of TRACP-stained osteoclasts derived from WT and Sbds-null mice after 6 days in culture with RANKL and M-CSF (both original magnification ×200). Significantly more large multinucleated osteoclasts were observed in WT cultures. (B) The marked difference in OCG between WT and SBDS-null cultures is visible to the eye. Shown are cultures derived from 3 separate WT (left) and Sbds-null (right) mice. (C) The number of osteoclasts and the number of nuclei per osteoclast were quantified. Sbds-null osteoclast cultures exhibited decreased OCG compared with WT cultures, as shown by significantly lower numbers of small (3 or 4 nuclei/osteoclast), medium (5-7 nuclei/osteoclast), and large (≥ 8 nuclei/osteoclast) osteoclasts (n = 8): $^*P < .01$. (D) Western blots showing that Sbds was deleted from Sbds-null monocytes. Levels of RANK and c-Fms between WT and Sbds-null cells were similar after 2 days of culture with RANKL and M-CSF. β-actin was used as a loading control. (E) There was no difference in osteoclast progenitor levels between WT and Sbds-null mice as measured by a colony-forming assay after 10 days in culture with M-CSF and RANKL (n = 3): $P > .05$. (F) Photomicrographs of TRACP-stained distal femoral bone sections at low magnification (original magnification ×100), and the boxed areas at high magnification (original magnification ×400), representative of more intense staining in WT sections. Osteoclasts were quantified in 3 bone sections per mouse and 3 mice per genotype (right). Significantly more small, medium and large osteoclasts were counted in WT sections (n = 3): $^*P < .001$; $^{**}P < .005$. (G) DXA analysis of age-matched female animals showed that WT mice had significantly higher BMD (top panel) and BMC (lower panel) in the whole body, lumbar vertebrae, and left femur than Sbds-null mice (n = 6): $^*P < .01$; $^{**}P < .005$.

measured first by their translocation into the nucleus. Osteoclasts were cultured for 6 days in 8-well chamber slides at 1×10^4 cells/well, and NF-κB and c-Jun localization was evaluated by immunostaining using an NF-κB and c-Jun activation kit (8400301, Thermo Scientific) following the manufacturer's directions and visualized by fluorescence microscopy (original magnification ×400, 40×/0.95 lens; Nikon Eclipse E1000). Images were taken and processed as described in "History and DXA analysis." Alternatively, RANK signaling was evaluated by measuring NF-κB and NFATc1 content in nuclear extracts isolated from WT and Sbds-null osteoclasts cultured after 4 days with M-CSF and in the absence or presence of RANKL. Nuclear extracts were obtained using a nuclear extract kit (Active Motif) following the manufacturer's directions, and protein concentrations were measured using the Bicinchoninic acid (BCA) method. Activation of NFATc1 was evaluated in 5 μg of nuclear extract by enzyme-linked immunosorbent assay (ELISA) using the TransAM NFATc1 transcription factor assay kit (Active Motif), which binds NFATc1 using a consensus binding sequence. Similarly, activation of NF-κB was measured in 0.5 μg of nuclear extract using the TransAM NF-κB p65 Chemi kit (Active Motif). Specificity of NFATc1 and NF-κB binding was assessed using the provided WT consensus and mutant oligonucleotide probes as competitors in the ELISA.

Quantitative real-time PCR

On days 2, 4, and 6 of OCG, RNA was extracted from WT and Sbds-null cultures (RNeasy mini kit, QIAGEN). Total RNA (500 ng) was reverse-transcribed into cDNA using Superscript II (Invitrogen) and Oligo-dT_{18}VN primer (ACGT). Primers were designed from the GenBank accession numbers NM_009007 for Rac1 (F5′-GAGACGGAGCTGTTGGTAAAA-3′; R5′-ATAGGCCCAGATTCACTGGTT-3′), NM_009008 for Rac2 (F5′-GACAGTAAGCCGGTGAACCTG-3′; R5′-CTGACTAGCGAGAAGCAGATG-3′), NM_007779 for c-Fms (F5′-TGTCATCGAGCCTAGTGGC-3′; R5′-CGGGAGATTCAGGGTCCAAG-3′), AF019046 for RANK (F5′-CTAATCCAGCAGGGAAGCAAAT-3′; R5′GACACGGGCATAGAGTCAGTTC-3′), AB109560 for DC-STAMP (F5′-TACGTGGAGAGAAGCAAGGAA-3′; R5′-ACACTGAGACGTGGTTTAGGAAT-3′), NM_009424 for TRAF6 (F5′-CCTTTCAGCGACCCACAATC-3′; R5′-ACTTCGTGGCTGGAAACCCT-3′), and M32599 for glyceraldehyde-3-phosphate dehydrogenase (F5′-CCTTCCGTGTTCCTACCCC-3′; R5′-GCCCAAGATGCCCTTCAGT-3′). A 1:10 cDNA dilution was used for all primer pairs to yield optimal PCR efficiency. Quantitative real-time (RT) PCR was performed in 20 μL reactions containing 5 μL diluted cDNA and 10 μL SsoFast EvaGreen Supermix (Bio-Rad) using the BioRad CFX96 Real Time System. Each reaction was performed in triplicate. PCR conditions were as follows: initial denaturation at 95°C for 30 seconds, annealing temperature at 60°C for 1 minute, extension at 72°C for 1 minute, repeated for 35 cycles. A final extension at 72°C for 10 minutes concluded the reaction. Data were normalized with internal glyceraldehyde-3-phosphate dehydrogenase control as previously described.[27]

Statistical analysis

For experiments in which there were multiple observations per sample, numerical results were expressed as mean ± SEM. For experiments in

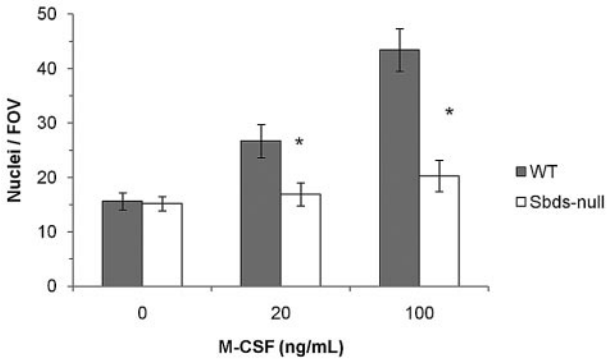

Figure 2. Sbds ablation results in decreased monocyte migration. Migration of monocytes was evaluated in a Boyden chamber assay and 2 concentrations of M-CSF as a chemoattractant. Sbds-null monocytes migrated significantly less versus WT monocytes at both 20 and100 ng/mL M-CSF (n = 5): $*P < .01$.

which there was only a single observation per sample, results were expressed as mean ± SD. Each experiment had a sample size of n ≥ 3. Statistical analysis was performed using Student *t* test. $P < .05$ was considered statistically significant.

Results

OCG is impaired in Sbds-ablated osteoclast progenitors

Sbds-null monocytes had a severe defect in forming osteoclasts in vitro. TRACP staining was clearly and significantly reduced in Sbds-null versus WT cultures (Figure 1A-C). Significantly reduced numbers of small (3 or 4 nuclei/cell), medium (5-7 nuclei/cell), and large osteoclasts (≥ 8 nuclei/cell) were generated from Sbds-null monocytes after 6 days in culture. Prolonging the number of days in culture to a total of 9 days did not increase the size or number of Sbds-null osteoclasts (not shown). To ensure that the conditional Sbds knockout did not affect important cellular characteristics limiting OCG, we measured the levels of osteoclast progenitors in a stem cell colony-forming assay as previously described,[28] and the receptors to the 2 essential cytokines RANKL and M-CSF, and RANK and c-Fms, respectively (Figure 1D-E). Sbds-null osteoclast progenitor levels were unchanged from WT levels, indicating unaffected cell proliferative activity, and RANK and c-Fms protein levels in early pre-osteoclasts after 2 days in culture were also unaltered. Thus, WT and Sbds-null pre-osteoclasts during early cell culture were quantitatively and qualitatively similar.

In vivo OCG was evaluated by TRACP staining of femoral histologic sections. Distal femur bone sections showed distinctly greater TRACP staining in WT sections and significantly higher numbers of multinucleated osteoclasts than in Sbds-null sections (Figure 1F). Phenotypically, WT and Sbds-null mice had similar body mass (22.0 ± 1.8 g and 20.5 ± 1.3 g, respectively; n = 6, $P > .05$), indicating no significant difference in growth and development. However, DXA analysis showed that both BMD and BMC were significantly reduced in Sbds-null mice as quantified in the whole skeleton and locally in the lumbar vertebra and left femur (Figure 1G). In addition, DXA showed that Sbds-null mice had significantly higher percentage body fat compared with WT littermates (28.8% ± 2.4% and 23.5% ± 1.7%, respectively; n = 6, $P < .005$).

Sbds regulates both migration and fusion of monocytes

Impaired osteoclast formation could have resulted from defective monocyte migration or fusion mechanisms, or both. We showed previously that migration of monocytes into close proximity of neighboring cells is an important step in OCG before fusion, and this process is controlled by multiple Rho GTPases.[27] Sbds-null monocytes migrated significantly less than WT monocytes at both 20 and100 ng/mL M-CSF (Figure 2). To measure whether Sbds-null monocytes also had a fusion defect, we cultured cells at both low and high initial plating densities, the rationale being that, if fusion mechanisms were unaffected in Sbds-null cells, osteoclast formation could be rescued (if Sbds-null monocytes were grown close together, ie, at high initial plating density). Significantly more

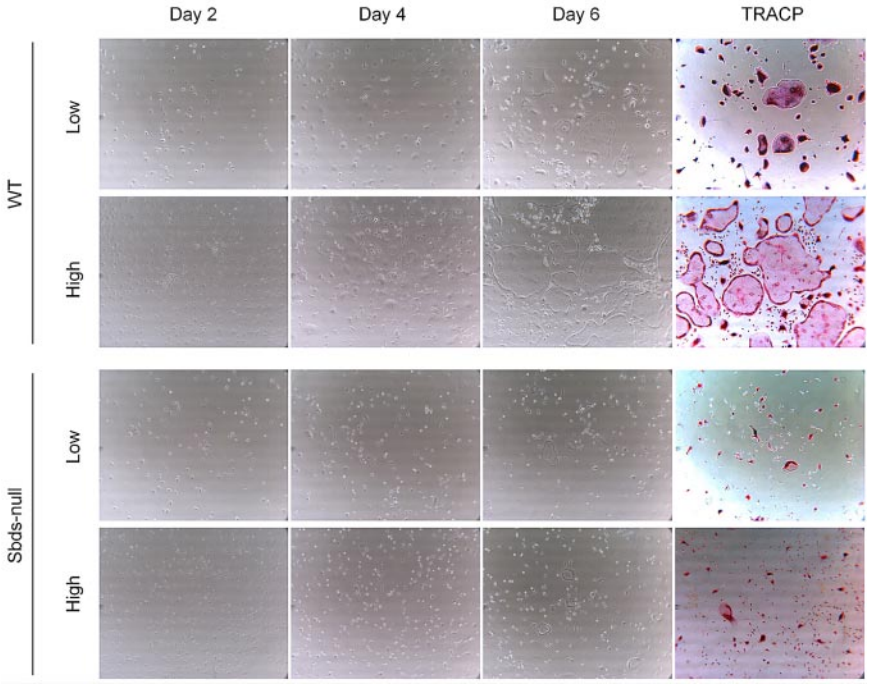

Figure 3. Sbds-null monocytes lack the ability to fuse even at high cell densities. Monocytes were cultured at 2 initial plating densities in 6-well plates, low (5×10^4 cells/well) and high (2.5×10^5 cells/well), to observe the effects of cell density on OCG. Representative photomicrographs (original magnification ×200) of WT (top 2 panels) and Sbds-null (lower 2 panels) cultures are shown on days 2, 4, and 6 of OCG, and representative TRACP-stained images of day 6 WT and Sbds-null cultures are shown on the right. At the 5-fold-higher initial plating density, WT cells formed clearly more large multinucleated osteoclasts than at the lower density. However, this increase in OCG was not observed for Sbds-null cells, suggestive of a fusion defect.

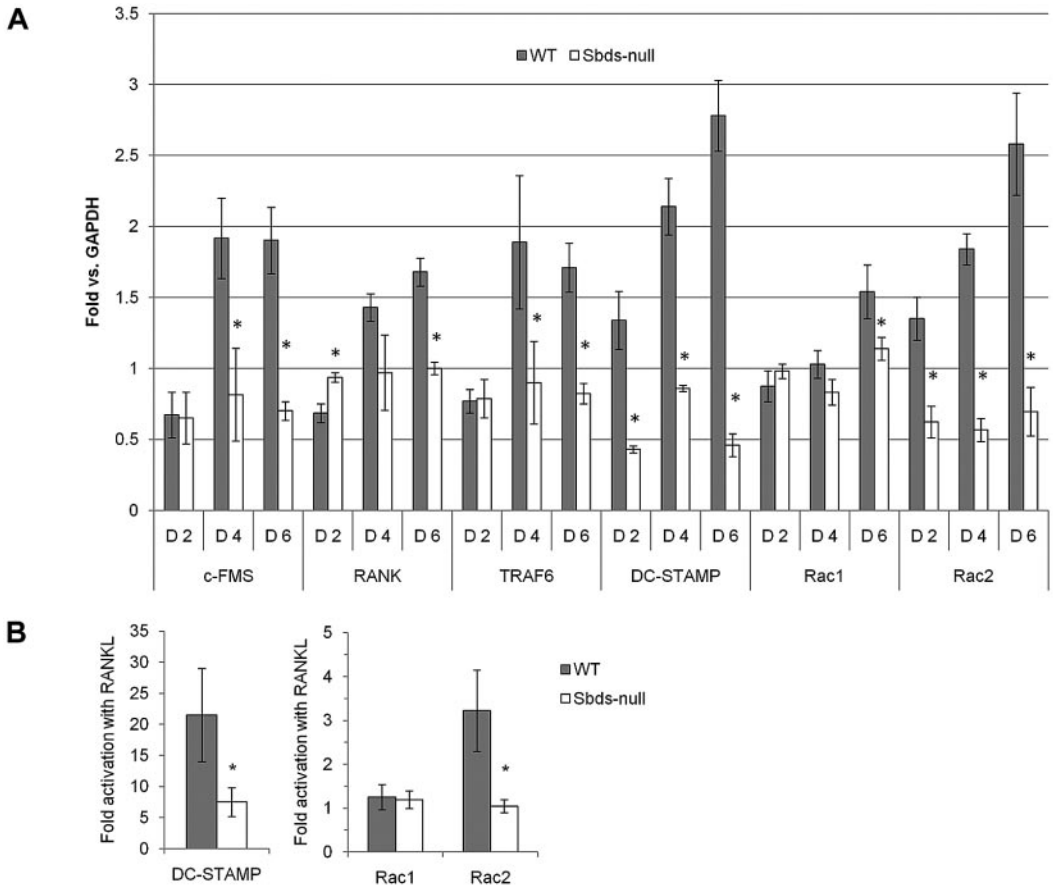

Figure 4. Sbds ablation results in the down-regulation of multiple genes important in OCG. (A) Quantitative real-time PCR was used to quantify gene expression on days 2, 4, and 6 of osteoclast cultures. Results are expressed as fold versus glyceraldehyde-3-phosphate dehydrogenase expression used as internal control. Sbds-null cells expressed significantly lower transcript levels of DC-STAMP and Rac2 on day 2 compared with WT cells, whereas expression of c-Fms, TRAF6, and Rac1 was unchanged. RANK expression was mildly increased in Sbds-null cells on day 2. All 6 genes were down-regulated by day 6 in Sbds-null cells; however, Rac1 was least affected at approximately 80% of WT levels (n = 3): $*P < .01$. (B) To examine whether Rac1 and Rac2 gene expression is RANKL-dependent, cells were cultured for 6 days in M-CSF alone or in combination with RANKL, and quantitative RT-PCR was performed. Results are expressed as fold activation in the presence of RANKL versus M-CSF alone, and compared with DC-STAMP expression, which is known to be RANKL-dependent. As expected, DC-STAMP was highly up-regulated by RANKL in WT cells, but this up-regulation was much less pronounced in Sbds-null cells. Rac1 gene expression was RANKL-independent; however, Rac2 was up-regulated 3.2-fold in WT cells but not in Sbds-null cells. Thus, Sbds-null cells exhibit defective RANK-mediated up-regulation of Rac2 and DC-STAMP (n = 3): $*P < .05$.

large, multinucleated osteoclasts were observed in WT cultures at the high concentration than at the low concentration (Figure 3). However, this was not observed in Sbds-null cells, and the number of multinucleated osteoclasts was similar when grown at either concentration. Thus, Sbds-null monocytes have both migration and fusion defects.

Sbds affects expression of genes crucial to OCG and actin dynamics

Expression of genes critical to OCG was examined by quantitative RT-PCR on days 2, 4, and 6 of culture (Figure 4A). These included the pre-osteoclast fusion receptor DC-STAMP, the cytokine receptors RANK and c-Fms, TRAF6 (the downstream binding adaptor protein of RANK), and the Rho GTPases Rac1 and Rac2 (both important in actin remodeling[33] and previously shown to be required for distinct aspects of OCG[28]). During early OCG (day 2), transcripts of membrane proteins involved in cell signaling (ie, RANK, c-Fms, and TRAF6) were similar between Sbds-null and WT cells. However, on days 4 and 6, expression of all 3 genes increased 2- to 3-fold in WT osteoclasts, although their expression in Sbds-null osteoclasts remained unchanged from day 2 levels, resulting in only 40% to 60% of WT levels by day 6. These results suggest impairment of osteoclast differentiation signaling. DC-STAMP transcripts doubled in WT cells between days 2 and 6; however, that of Sbds-null cells was consistently lower and remained at less than 20% of WT levels on day 6. Reduced DC-STAMP expression could explain the fusion defect observed in Sbds-null cells. Rac1 transcript levels were similar between WT and Sbds-null cells on days 2 and 4 but decreased slightly to 80% of WT levels by day 6 in Sbds-null cells. Meanwhile, Rac2 levels were notably decreased in Sbds-null osteoclasts throughout the course of osteoclast formation, with only 40% on day 2 and less than 20% of WT levels by day 6.

We suspected deficient RANK signaling in Sbds-null osteoclasts because of decreased RANK and TRAF6 transcripts and the failure to up-regulate DC-STAMP. Because there was a mild decrease in Rac1 and a severe decrease in Rac2, we investigated whether their gene expression is mediated by RANKL stimulation as an explanation to their decreased expression. Cells were cultured for 6 days with M-CSF and in the presence and absence of RANKL, and gene expression was compared with that of DC-STAMP, which is known to be up-regulated by RANKL (Figure 4B). Both DC-STAMP, and surprisingly Rac2, were significantly up-regulated by RANKL in WT cells by 21-fold and 3.2-fold, respectively, whereas in Sbds-null cells DC-STAMP only increased 7-fold and Rac2 remained unchanged.

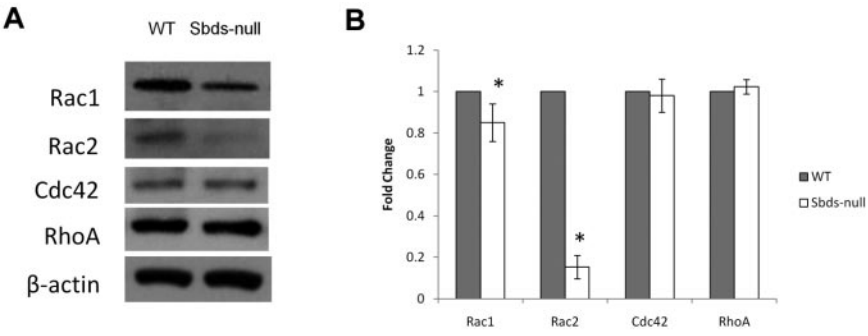

Figure 5. Quantification of Rho GTPase levels important in regulating actin dynamics and migration. Rho GTPase protein levels were analyzed on day 6 by Western blotting. (A) Sbds-null cells expressed slightly lower Rac1, and greatly reduced Rac2 levels versus WT cells. Levels of Cdc42 and RhoA were unchanged between WT and Sbds-null cells. Band intensities were normalized to β-actin used as loading control. (B) Quantification of band intensities by densitometry illustrating slightly reduced Rac1 and greatly reduced Rac2 levels (n = 4): $*P < .01$.

Conversely, Rac1 gene expression was not increased significantly with RANKL costimulation versus M-CSF alone in either cell type (~ 1.2-fold for both, $P > .05$). These results show that Sbds-null cells exhibit an impaired up-regulation of RANKL-dependent DC-STAMP and Rac2, whereas Rac1 gene expression is RANKL independent.

To verify decreased Rac during normal OCG, we measured protein levels of Rac1 and Rac2 on day 6 of osteoclast cultures (Figure 5). Sbds-null osteoclasts expressed mildly reduced Rac1 and severely reduced Rac2 protein levels (85% and < 20% of WT, respectively), confirming the decreased transcript levels observed. Evaluation of 2 other members of the Rho GTPase family not directly involved with osteoclast differentiation, Cdc42 and RhoA, showed unchanged levels between WT and Sbds-null osteoclasts.

Rescuing impaired migration and OCG by Rac1/Rac2 supplementation

A major role for Rho GTPases is to regulate the actin cytoskeleton during cellular migration.[33] We have already shown that Rac2 is the major Rho GTPase that was down-regulated in Sbds-null osteoclasts. Previously, we successfully used TAT fusion proteins tethered to Rho GTPases to rescue impaired migration.[27] To determine whether addition of exogenous Rac2 could rescue migration in Sbds-null monocytes, we added TAT proteins fused to either wild-type Rac2 (Rac2-WT) or constitutively active Rac2 (Rac2-CA) (Figure 6A). Only Rac2-CA increased basal WT monocyte migration in the absence of M-CSF, and neither Rac2-CA nor Rac2-WT further increased WT monocyte migration in the presence of M-CSF. In Sbds-null monocytes, Rac2-CA increased basal migration slightly, but in the presence of M-CSF both Rac2-CA and Rac2-WT significantly rescued migration to nearly WT levels. Further supplementation of Sbds-null monocytes with Rac1-CA in conjunction with Rac2-CA did not further improve their migratory ability.

Although Sbds-null monocyte migration was nearly fully rescued by supplementation of Rac2, OCG was not. Addition of the same concentrations of Rac2 TAT fusion proteins that rescued migration did not increase pre-osteoclast fusion (Figure 6B).

Sbds is required for activation of osteoclast transcription factors downstream of RANK

Because expression of RANK and TRAF6 was reduced in Sbds-null osteoclasts on days 4 and 6 of OCG, and there was a partial to total failure in the up-regulation of RANKL-dependent DC-STAMP and Rac2, we evaluated whether signaling downstream of RANK was impaired in Sbds-null osteoclasts after 6 days in culture. Nuclear localization of NF-κB, a marker of RANK activation, was analyzed using fluorescence microscopy (Figure 7A). Both large and small WT multinucleated osteoclasts showed clear nuclear localization of NF-κB indicative of its active status and intact RANK signaling. However, NF-κB staining was cytoplasmic in Sbds-null cells. Similar results were observed on day 4 (not shown). Staining for c-Jun, a transcription factor that mediates the antiapoptotic effect of RANKL in osteoclasts[34] but not directly downstream of RANK or absolutely required for OCG,[35] was

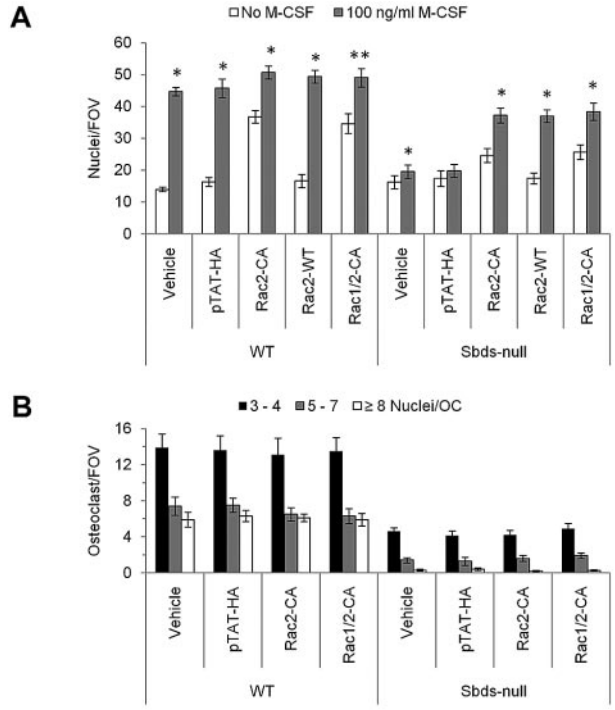

Figure 6. Supplementation of Sbds-null monocytes with Rac2 TAT fusion proteins rescues migration but not OCG. (A) Migration of Sbds-null monocytes toward 100 ng/mL M-CSF was rescued by preincubating cells with WT or CA Rac2 TAT fusion proteins before the migration assay. Addition of the empty vector (pTAT-HA) had no effect on migration of WT or Sbds-null monocytes. Only Rac2-CA increased basal WT monocyte migration in the absence of M-CSF, and neither Rac2-CA nor Rac2-WT appreciably further increased WT monocyte migration in the presence of M-CSF. Rac2-CA mildly increased basal SBDS-null monocyte migration, and in the presence of M-CSF both Rac2-CA and Rac2-WT increased Sbds-null monocyte migration to nearly WT levels. Cosupplementation of cells with equimolar Rac1-CA and Rac2-CA (Rac1/2-CA) did not further increase migration of WT or Sbds-null monocytes in the presence or absence of M-CSF over and above levels achieved by Rac2-CA alone. Statistical significance was measured by comparing the number of monocytes that migrated in the presence of M-CSF to resting values within each treatment group (n ≥ 3): $*P < .005$; $**P < .01$. (B) OCG was not rescued in Sbds-null cultures treated with Rac2-CA or Rac1/2-CA at concentrations that increased migration. Small (3 or 4 nuclei/OC), medium (5-7 nuclei/OC), and large (≥ 8 nuclei/OC) osteoclasts were quantified after TRACP staining. In both genotypes, there was no difference in the number of osteoclasts in each size category after treatments by pTAT-HA, Rac2-CA, or Rac1/2-CA versus vehicle alone (n = 4): $P > .05$.

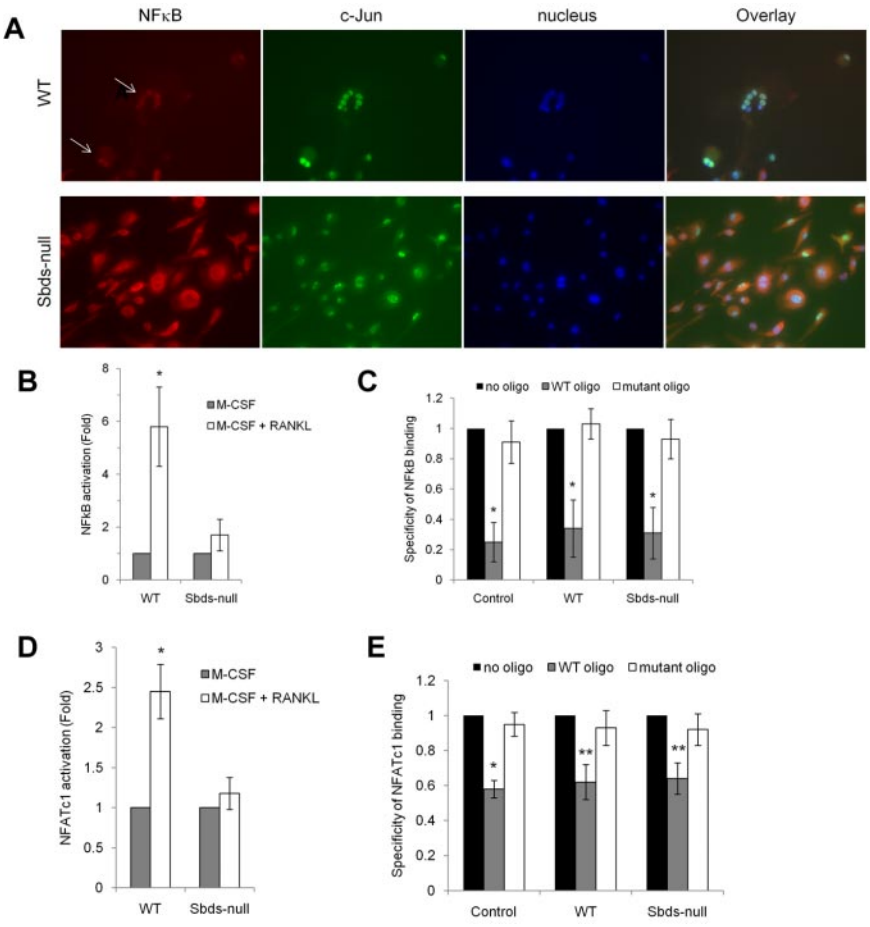

Figure 7. Sbds ablation is associated with impaired RANK signaling. (A) Signaling downstream of RANK was evaluated by immunostaining for NF-κB on day 6 of OCG. NF-κB was found to be activated only in WT osteoclasts as shown by its exclusively nuclear distribution (arrows). Sbds-null osteoclasts did not exhibit active NF-κB as shown by its cytoplasmic distribution. Both Sbds-null and WT osteoclasts demonstrated activated, nuclear c-Jun, a transcription factor not directly involved in RANK signaling in osteoclasts. The staining pattern was identical in day 4 osteoclasts. (B) Alternatively, activation of NF-κB was measured by performing an ELISA on NF-κB content in nuclear extracts of day 4 osteoclasts. Stimulation of WT cells by M-CSF and RANKL resulted in a significant 5.8-fold increase in nuclear NF-κB signal versus stimulation by M-CSF alone (n = 4): $*P < .005$. There was an insignificant increase in nuclear NF-κB signal after stimulation of Sbds-null cells with M-CSF and RANKL: $P = .065$. (C) Specificity of the NF-κB ELISA was verified with the addition of WT or mutant oligonucleotide competitors. WT oligo, representing the native consensus binding sequence of NF-κB (5′-GGGACTTTCC-3′), significantly inhibited NF-κB binding in the positive control (Jurkat cells stimulated with PMA and A23187), WT and Sbds-null nuclear extracts, whereas the mutant consensus oligonucleotide had no effect. Specificity of 1 signifies 100% specificity (n = 4): $*P < .01$. (D) Translocation of NFATc1 into the nucleus was evaluated as a second marker of the RANK signaling pathway by performing an ELISA on NFATc1 content in day 4 nuclear extracts. Stimulation of WT cells by M-CSF and RANKL resulted in a significant 2.5-fold increase in nuclear NFATc1 signal versus stimulation by M-CSF alone. There was no increase in nuclear NFATc1 signal after stimulation of Sbds-null cells with M-CSF and RANKL (n = 4): $*P < .005$. (E) NFATc1 ELISA showed good specificity as the WT oligo, representing the native consensus binding sequence of NFATc1 (5′-AGGAAA-3′), significantly inhibited NFATc1 binding in the positive control (leukoagglutinin-stimulated Jurkat cells), WT and Sbds-null nuclear extracts, whereas the mutant consensus oligonucleotide had no effect (n = 4): $*P < .005$; $**P < .01$.

nuclear in both WT and Sbds-null cells, illustrating that cell signaling in an unrelated pathway was not affected.

As further evidence of disturbed RANK signaling, activation of NF-κB and NFATc1, another RANKL-dependent transcription factor crucial for OCG, was assessed in nuclear extracts purified from day 4 osteoclasts by ELISA (Figure 7B,D). Under RANKL costimulation, WT nuclear extracts had a 5.8-fold increase in NF-κB binding and 2.5-fold increase in NFATc1 binding compared with WT cells cultured with M-CSF only. There was no appreciable increase in NF-κB or NFATc1 content in nuclear extracts of Sbds-null osteoclasts with RANKL costimulation. Specificity of NF-κB and NFATc1 binding was confirmed by the ablated signal only in the presence of WT and not the mutant consensus oligonucleotide competitor (Figure 7C,E). Thus, impaired activation of NF-κB and NFATc1 transcription factors reflects an uncoupling of 2 divergent arms of signaling downstream of RANK.

Discussion

The spectrum of abnormalities, including the hematologic issues present in SDS, have been of interest for some time; however, mechanisms underlying the more recent observations of skeletal dysplasias have not been well studied. Although SBDS is ubiquitously expressed, SDS defects are relatively organ specific (ie, pancreas, liver, bone marrow, and bone). Osteoclasts, cells responsible for bone remodeling through resorption, could potentially contribute to disruptions in bone homeostasis, resulting in abnormalities observed in bones of SDS patients. Because global deletion of Sbds in mice results in early embryonic lethality,[17] we used a Cre-Lox conditional knock-out strategy in which Sbds was deleted from cells of the myeloid lineages only (monocyte/macrophage and neutrophils) to generate viable mice that enabled us to study OCG both in vitro and in vivo.

Sbds is required for OCG

We show that Sbds was required for the formation of large, multinucleated osteoclasts not only in vitro, but also in vivo. An earlier report showed a requirement for SBDS in maintaining viability of granulocyte precursors as SBDS knocked-down neutrophilic cells experienced increased apoptosis.[36] However, others reported that SBDS was required for differentiation but not proliferation of primary mouse hematopoietic progenitors.[37] We found that osteoclast precursor proliferation is independent of Sbds, and early Sbds-null pre-osteoclasts were qualitatively similar to WT pre-osteoclasts, as evidenced by similar expression of RANK and c-Fms on day 2. We therefore investigated potential mechanisms that could cause impaired osteoclast differentiation in Sbds-null osteoclast precursors.

Migration is impaired in Rac2-deficient Sbds-ablated cells

In addition to experiencing neutropenia, SDS neutrophils have chemotatic defects characterized by inabilities to orient toward a spatial chemoattractant gradient and to polarize.[21,22] The SBDS homolog in *Dictyostelium discoideum*, an amoeba model to study neutrophils, is enriched in pseudopods of migrating cells,[38] further implicating a role for SBDS in chemotaxis. Migration of monocytes/

pre-osteoclasts into close proximity before fusion is an important step in OCG,[24] and we have shown previously that defective migration alone could contribute to decreased osteoclast formation.[27] Ablation of Sbds in monocytes resulted in impaired migration toward even the highest concentration of M-CSF used. We have shown that defective activation of multiple Rho GTPases (ie, Rac1, Cdc42 and RhoA) was responsible for impaired monocyte migration.[27] Moreover, previous studies have demonstrated that Rac2-deficient neutrophils exhibit defective chemotaxis.[39,40] As normal actin dynamics that is regulated by Rho GTPases is required for cellular migration/chemotaxis,[33] we investigated whether members of the Rho GTPase family were deficient in quantity or defective in their activation. RhoA and Cdc42 protein levels in day 6 Sbds-null cultures were unaffected, whereas Rac1 was only mildly reduced and Rac2 was severely reduced. Unexpectedly, we found that in WT cells Rac2 mRNA was up-regulated by RANKL costimulation, although no appreciable increase was observed with Rac1. Although both the closely related Rac1 and Rac2 have been shown to be required for OCG,[28] it is interesting that only Rac2 is downstream of RANK. We have unpublished data that in RAW264.7 cells, Rac2 expression was up-regulated by RANKL stimulation at the mRNA and protein level whereas Rac1 expression remained constant. Others have also shown the RANKL-dependent up-regulation of Rac2 at the transcript level in bone marrow-derived osteoclasts and RAW cells.[41] Because RANK signaling is impaired in Sbds-null cells (see next section), it is probable that Rac2 expression does not reach adequate levels to regulate migration. The fact that Rac1 is not downstream of RANK also explains its relatively normal expression level despite RANK signaling impairment.

To clarify the role of Rac2 in monocyte migration, we rescued migration-defective, Rac2-deficient Sbds-null cells with TAT-Rac2 fusion proteins. TAT is an 11-amino acid peptide derived from HIV that we and others[27,31,32] have used to transduce difficult-to-transfect primary cells, including monocytes and osteoclasts. We observed that migration was nearly fully rescued by either Rac2-WT or Rac2-CA, demonstrating the requirement for Rac2 in association with Sbds in monocyte migration and that the migration defect was the result of decreased Rac2 expression in Sbds-null cells, not in its activation. Our results are supported by others[21] who showed that in neutrophilic PLB-985 cells, F-actin, SBDS, and Rac2 colocalized in cellular protrusions after stimulation, and SDS neutrophils exhibited disturbed F-actin polymerization and delayed polarization, suggesting SBDS and Rac2 may play an interdependent regulatory role in controlling actin dynamics required for directed migration. Moreover, Rac2 had been shown to regulate cofilin dephosphorylation and ARP2/3 de novo nucleation important in actin free-barbed end generation, required for leading edge protrusion in cells undergoing chemotaxis.[42] Thus, multiple lines of evidence point to a role for Rac2 in conjunction with SBDS in regulating monocyte migration. Rac1 cosupplementation did not result in further augmentation of migration in Sbds-null monocytes, probably resulting from adequate native Rac1 levels to meet the minimum threshold required for migration. In recent studies,[18,19] SBDS has been shown to be localized to, and stabilize mitotic spindles in, human myeloid progenitors and bone marrow stromal cells, and bound to microtubules in in vitro binding studies, suggesting a role for SBDS in cell division. As microtubules are intricately linked with the actin cytoskeleton and actin-rich podosomes in osteoclasts, SBDS may additionally mediate actin dynamics via interactions with microtubules.

Sbds regulates genes important in pre-osteoclast differentiation and fusion

We investigated impairments in cell signaling, differentiation, and expression of the required cytokine/fusion receptors and adaptor intermediates as potential causes for impaired migration and fusion. A major signaling axis for OCG is the RANK-TRAF6-NF-κB axis, which requires the major differentiation cytokine RANKL for activation. RANKL-RANK binding is followed by the recruitment of adaptor molecule TRAF6 to the cytoplasmic tail of RANK and subsequent downstream activation of transcription factors NF-κB and c-Fos, the latter within the activator protein-1 complex.[43] Reduced RANK and TRAF6 expression in Sbds-null cells on days 4 and 6 probably contributed to reduced signal transduction along this axis required for osteoclast differentiation, fusion, and maturation. Moreover, in addition to being the main proliferation factor, M-CSF functions secondarily as a differentiation factor for osteoclasts[44]; therefore, although c-Fms signaling is not downstream of RANK, decreased c-Fms expression could have had additive deleterious effects on osteoclast differentiation. Impaired RANK signaling was confirmed by greatly reduced NF-κB activation in Sbds-null osteoclasts. A second major transcription factor crucial for OCG is NFATc1. Activation of NFATc1, a RANKL-dependent transcription factor that is up-regulated in later-stage osteoclast differentiation via Ca^{2+}/calcineurin,[35] was also impaired in Sbds-null cells, further evidence that RANK signaling was disturbed. Finally, Rac2 expression, which we show to be regulated by RANK, was severely low in Sbds-null cells, which ultimately prevented effective migration.

Without adequate activation of NF-κB and NFATc1, crucial genes for OCG are not turned on, of which DC-STAMP is one example. Expression of DC-STAMP, the crucial fusion receptor absolutely required for osteoclast multinucleation[45] and normally up-regulated by RANKL,[46] was low in Sbds-null cells on day 2 and was reduced by more than 5-fold versus WT on day 6. Down-regulation of DC-STAMP in Sbds-null cells probably resulted from impaired RANK signaling; this alone could explain the inability to rescue pre-osteoclast fusion by increasing cell plating density, as well as by supplementation with TAT proteins as this would not be expected to correct the deficiency in DC-STAMP expression. Hesling et al[47] showed that, in HEK293 cells, SBDS knock down resulted in both up- and down-regulation of genes required for brain, skeletal, and blood cell development. Importantly, *FOS*, one of 2 major components of the activator protein-1 complex that becomes activated during OCG, saw a 5.3-fold decrease in transcript level. Thus, it appears that Sbds has pleiotropic effects on the regulation of certain genes, without which subsequent osteoclast differentiation and fusion become blocked. We observed that activation of c-Jun, an antiapoptotic mediator of RANKL in osteoclasts and a nonessential transcription factor in OCG, was not impaired in Sbds-null cells, indicating only select signaling pathways were affected. Interestingly, HeLa cells depleted of SBDS exhibited a 3- to 6-fold increase in mRNA and secreted protein levels of OPG, a decoy RANKL receptor.[48] Whether Sbds-null pre-osteoclasts intrinsically produce OPG to sequester RANKL, thus preventing RANK activation leading to decreased OCG, awaits further investigation.

Linking Sbds with bone homeostasis in SDS

The activities of bone-producing osteoblasts must be kept in balance with that of bone-resorbing osteoclasts to maintain homeostasis. Osteoblast activity in excess of balanced osteoclast

activity results in osteopetrosis, although the opposite leads to osteoporosis. A recent study[9] of 11 SDS patients showed they exhibit low-turnover osteoporosis characterized by low bone mass (decreased BMD and BMC), reduced bone turnover, reduced numbers of osteoclasts, osteoblasts and osteoid, and vertebral fragility. These results corroborate with earlier findings of generalized osteopenia and early osteoporotic vertebral deformities in SDS patients.[8] We show that the Sbds-null mouse phenotype accurately recapitulates those findings of SDS patients (ie, decreased BMD, BMC, and in vivo OCG). It may be counterintuitive that decreased in vivo OCG produces an osteoporotic phenotype, as the opposite would be expected. Moreover, several murine models in which OCG is either severely inhibited or altogether absent (eg, gene mutations in M-CSF, PU.1, or RANKL) result in overt osteopetrosis.[26,49,50] This can be explained by the complete uncoupling of bone remodeling homeostasis as a result of the nonphysiologic, severe impairment in bone resorption, resulting in net bone deposition. In our study, numbers of multinucleated, TRACP-positive osteoclasts, although decreased, were still present in vivo; thus, we hypothesize that there was an overcompensation in the decrease of osteoblast activity, resulting in a net loss of BMC/BMD, and osteoporosis. Interestingly, osteoblasts and adipocytes are derived from the same mesenchymal stem cells, with Runx2 and PPARγ driving the osteoblast and adipocyte lineages, respectively,[51,52] and the numbers of each cell type share an inverse relationship.[51,53] Thus, the incidental finding of increased adipogenesis in Sbds-null mice is indirect evidence of decreased osteoblastogenesis and a resultant push toward the adipocyte lineage during stem cell differentiation. This is supported by previous work from our laboratory where a filamin A targeted knockout to granulocytes resulted in decreased in vitro and in vivo OCG and a mild osteoporotic phenotype resulting from decreased bone formation, as measured by decreases in bone formation markers, such as serum osteocalcin and alkaline phosphatase activity of osteoblast progenitor cells.[27] The dysregulation in the crosstalk between osteoclasts and osteoblasts in Sbds-null mice awaits planned future osteogenic and histomorphometric studies. It follows that decreased OCG in SDS patients could potentially contribute to an imbalance in bone homeostasis, resulting in an associated compensatory decrease in osteoblastogenesis and the array of skeletal abnormalities observed. This study was the first to evaluate osteoclast formation in SDS and validates an animal model to study osteoclast dysfunction in SDS. The evidence presented on Sbds ablation illustrates impaired monocyte migration resulting from a failure in RANKL-mediated up-regulation of Rac2 and impaired signaling downstream of RANK, resulting in decreased pre-osteoclast differentiation and OCG.

Acknowledgments

This work was supported by the Canadian Institutes of Health Research (research grant MOP-81265). M.G. is supported by the Canadian Institutes of Health Research (New Investigator Award). R.L. is supported by the Canadian Institutes of Health Research (Bisby Fellowship) and is a Canadian Institutes of Health Research Strategic Training Fellow (STP-53877).

Authorship

Contribution: R.L. designed and performed research, collected analyzed, and interpreted data, performed statistical analysis, and wrote and revised the manuscript; K.C. performed research, collected and analyzed data, and performed statistical analysis; Y.W. designed research and analyzed data; J.R. contributed vital tools (bred transgenic mice), analyzed data, and wrote the manuscript; and M.G. designed research; analyzed data, and wrote the manuscript.

Conflict-of-interest disclosure: The authors declare no competing financial interests.

Correspondence: Michael Glogauer, 150 College St, Rm 221, Toronto, ON M5S 3E2; Canada; e-mail: michael.glogauer@utoronto.ca.

References

1. Shwachman H, Diamond LK, Oski FA, Khaw KT. The syndrome of pancreatic insufficiency and bone marrow dysfunction. *J Pediatr.* 1964;65:645-663.
2. Bodian M, Sheldon W, Lightwood R. Congenital hypoplasia of the exocrine pancreas. *Acta Paediatr.* 1964;53:282-293.
3. Ginzberg H, Shin J, Ellis L, et al. Segregation analysis in Shwachman-Diamond syndrome: evidence for recessive inheritance. *Am J Hum Genet.* 2000;66(4):1413-1416.
4. Shimamura A. Inherited bone marrow failure syndromes: molecular features. *Hematology Am Soc Hematol Educ Program.* 2006:63-71.
5. Aggett PJ, Cavanagh NP, Matthew DJ, Pincott JR, Sutcliffe J, Harries JT. Shwachman's syndrome: a review of 21 cases. *Arch Dis Child.* 1980;55(5):331-347.
6. Ginzberg H, Shin J, Ellis L, et al. Shwachman syndrome: phenotypic manifestations of sibling sets and isolated cases in a large patient cohort are similar. *J Pediatr.* 1999;135(1):81-88.
7. Mack DR, Forstner GG, Wilschanski M, Freedman MH, Durie PR. Shwachman syndrome: exocrine pancreatic dysfunction and variable phenotypic expression. *Gastroenterology.* 1996;111(6):1593-1602.
8. Makitie O, Ellis L, Durie PR, et al. Skeletal phenotype in patients with Shwachman-Diamond syndrome and mutations in SBDS. *Clin Genet.* 2004;65(2):101-112.
9. Toiviainen-Salo S, Mayranpaa MK, Durie PR, et al. Shwachman-Diamond syndrome is associated with low-turnover osteoporosis. *Bone.* 2007;41(6):965-972.
10. Ho W, Cheretakis C, Durie P, Kulkarni G, Glogauer M. Prevalence of oral diseases in Shwachman-Diamond syndrome. *Spec Care Dentist.* 2007;27(2):52-58.
11. Boocock GR, Morrison JA, Popovic M, et al. Mutations in SBDS are associated with Shwachman-Diamond syndrome. *Nat Genet.* 2003;33(1):97-101.
12. Savchenko A, Krogan N, Cort JR, et al. The Shwachman-Bodian-Diamond syndrome protein family is involved in RNA metabolism. *J Biol Chem.* 2005;280(19):19213-19220.
13. Menne TF, Goyenechea B, Sanchez-Puig N, et al. The Shwachman-Bodian-Diamond syndrome protein mediates translational activation of ribosomes in yeast. *Nat Genet.* 2007;39(4):486-495.
14. Rujkijyanont P, Adams SL, Beyene J, Dror Y. Bone marrow cells from patients with Shwachman-Diamond syndrome abnormally express genes involved in ribosome biogenesis and RNA processing. *Br J Haematol.* 2009;145(6):806-815.
15. Austin KM, Leary RJ, Shimamura A. The Shwachman-Diamond SBDS protein localizes to the nucleolus. *Blood.* 2005;106(4):1253-1258.
16. Ganapathi KA, Austin KM, Lee CS, et al. The human Shwachman-Diamond syndrome protein, SBDS, associates with ribosomal RNA. *Blood.* 2007;110(5):1458-1465.
17. Zhang S, Shi M, Hui CC, Rommens JM. Loss of the mouse ortholog of the shwachman-diamond syndrome gene (Sbds) results in early embryonic lethality. *Mol Cell Biol.* 2006;26(17):6656-6663.
18. Austin KM, Gupta ML, Coats SA, et al. Mitotic spindle destabilization and genomic instability in Shwachman-Diamond syndrome. *J Clin Invest.* 2008;118(4):1511-1518.
19. Orelio C, Verkuijlen P, Geissler J, van den Berg TK, Kuijpers TW. SBDS expression and localization at the mitotic spindle in human myeloid progenitors. *PLoS One.* 2009;4(9):e7084.
20. Ball HL, Zhang B, Riches JJ, et al. Shwachman-Bodian Diamond syndrome is a multi-functional protein implicated in cellular stress responses. *Hum Mol Genet.* 2009;18(19):3684-3695.
21. Orelio C, Kuijpers TW. Shwachman-Diamond syndrome neutrophils have altered chemoattractant-induced F-actin polymerization and polarization characteristics. *Haematologica.* 2009;94(3):409-413.
22. Stepanovic V, Wessels D, Goldman FD, Geiger J,

Soll DR. The chemotaxis defect of Shwachman-Diamond Syndrome leukocytes. *Cell Motil Cytoskeleton.* 2004;57(3):158-174.

23. Sims NA, Gooi JH. Bone remodeling: multiple cellular interactions required for coupling of bone formation and resorption. *Semin Cell Dev Biol.* 2008;19(5):444-451.
24. Chen EH, Grote E, Mohler W, Vignery A. Cell-cell fusion. *FEBS Lett.* 2007;581(11):2181-2193.
25. Boyle WJ, Simonet WS, Lacey DL. Osteoclast differentiation and activation. *Nature.* 2003; 423(6937):337-342.
26. Kong YY, Yoshida H, Sarosi I, et al. OPGL is a key regulator of osteoclastogenesis, lymphocyte development and lymph-node organogenesis. *Nature.* 1999;397(6717):315-323.
27. Leung R, Wang Y, Cuddy K, et al. Filamin A regulates monocyte migration through Rho small GTPases during osteoclastogenesis. *J Bone Miner Res.* 25(5):1077-1091.
28. Wang Y, Lebowitz D, Sun C, Thang H, Grynpas MD, Glogauer M. Identifying the relative contributions of Rac1 and Rac2 to osteoclastogenesis. *J Bone Miner Res.* 2008;23(2):260-270.
29. Clausen BE, Burkhardt C, Reith W, Renkawitz R, Forster I. Conditional gene targeting in macrophages and granulocytes using LysMcre mice. *Transgenic Res.* 1999;8(4):265-277.
30. Ye M, Iwasaki H, Laiosa CV, et al. Hematopoietic stem cells expressing the myeloid lysozyme gene retain long-term, multilineage repopulation potential. *Immunity.* 2003;19(5):689-699.
31. Dolgilevich S, Zaidi N, Song J, Abe E, Moonga BS, Sun L. Transduction of TAT fusion proteins into osteoclasts and osteoblasts. *Biochem Biophys Res Commun.* 2002;299(3):505-509.
32. Zhang H, Sun C, Glogauer M, Bokoch GM. Human neutrophils coordinate chemotaxis by differential activation of Rac1 and Rac2. *J Immunol.* 2009;183(4):2718-2728.
33. Jaffe AB, Hall A. Rho GTPases: biochemistry and biology. *Annu Rev Cell Dev Biol.* 2005;21:247-269.
34. Ikeda F, Matsubara T, Tsurukai T, Hata K, Nishimura R, Yoneda T. JNK/c-Jun signaling mediates an anti-apoptotic effect of RANKL in osteoclasts. *J Bone Miner Res.* 2008;23(6):907-914.
35. Negishi-Koga T, Takayanagi H. Ca2+-NFATc1 signaling is an essential axis of osteoclast differentiation. *Immunol Rev.* 2009;231(1):241-256.
36. Yamaguchi M, Fujimura K, Toga H, Khwaja A, Okamura N, Chopra R. Shwachman-Diamond syndrome is not necessary for the terminal maturation of neutrophils but is important for maintaining viability of granulocyte precursors. *Exp Hematol.* 2007;35(4):579-586.
37. Rawls AS, Gregory AD, Woloszynek JR, Liu F, Link DC. Lentiviral-mediated RNAi inhibition of Sbds in murine hematopoietic progenitors impairs their hematopoietic potential. *Blood.* 2007;110(7): 2414-2422.
38. Wessels D, Srikantha T, Yi S, Kuhl S, Aravind L, Soll DR. The Shwachman-Bodian-Diamond syndrome gene encodes an RNA-binding protein that localizes to the pseudopod of Dictyostelium amoebae during chemotaxis. *J Cell Sci.* 2006; 119(2):370-379.
39. Ambruso DR, Knall C, Abell AN, et al. Human neutrophil immunodeficiency syndrome is associated with an inhibitory Rac2 mutation. *Proc Natl Acad Sci U S A.* 2000;97(9):4654-4659.
40. Carstanjen D, Yamauchi A, Koornneef A, et al. Rac2 regulates neutrophil chemotaxis, superoxide production, and myeloid colony formation through multiple distinct effector pathways. *J Immunol.* 2005;174(8):4613-4620.
41. Rho J, Altmann CR, Socci ND, et al. Gene expression profiling of osteoclast differentiation by combined suppression subtractive hybridization (SSH) and cDNA microarray analysis. *DNA Cell Biol.* 2002;21(8):541-549.
42. Sun CX, Magalhaes MA, Glogauer M. Rac1 and Rac2 differentially regulate actin free barbed end formation downstream of the fMLP receptor. *J Cell Biol.* 2007;179(2):239-245.
43. Wada T, Nakashima T, Hiroshi N, Penninger JM. RANKL-RANK signaling in osteoclastogenesis and bone disease. *Trends Mol Med.* 2006;12(1): 17-25.
44. Asagiri M, Takayanagi H. The molecular understanding of osteoclast differentiation. *Bone.* 2007; 40(2):251-264.
45. Yagi M, Miyamoto T, Sawatani Y, et al. DC-STAMP is essential for cell-cell fusion in osteoclasts and foreign body giant cells. *J Exp Med.* 2005;202(3):345-351.
46. Kukita T, Wada N, Kukita A, et al. RANKL-induced DC-STAMP is essential for osteoclastogenesis. *J Exp Med.* 2004;200(7):941-946.
47. Hesling C, Oliveira CC, Castilho BA, Zanchin NI. The Shwachman-Bodian-Diamond syndrome associated protein interacts with HsNip7 and its down-regulation affects gene expression at the transcriptional and translational levels. *Exp Cell Res.* 2007;313(20):4180-4195.
48. Nihrane A, Sezgin G, Dsilva S, et al. Depletion of the Shwachman-Diamond syndrome gene product, SBDS, leads to growth inhibition and increased expression of OPG and VEGF-A. *Blood Cells Mol Dis.* 2009;42(1):85-91.
49. Yoshida H, Hayashi S, Kunisada T, et al. The murine mutation osteopetrosis is in the coding region of the macrophage colony stimulating factor gene. *Nature.* 1990;345(6274):442-444.
50. Tondravi MM, McKercher SR, Anderson K, et al. Osteopetrosis in mice lacking haematopoietic transcription factor PU.1. *Nature.* 1997;386(6620): 81-84.
51. Kawaguchi H. Molecular backgrounds of age-related osteoporosis from mouse genetics approaches. *Rev Endocr Metab Disord.* 2006;7(1): 17-22.
52. Pittenger MF, Mackay AM, Beck SC, et al. Multilineage potential of adult human mesenchymal stem cells. *Science.* 1999;284(5411):143-147.
53. Castro CH, Shin CS, Stains JP, et al. Targeted expression of a dominant-negative N-cadherin in vivo delays peak bone mass and increases adipogenesis. *J Cell Sci.* 2004;117(13):2853-2864.